Nanocomposites of Polyhedral Oligomeric Phenethylsilsesquioxanes and Poly(bisphenol A carbonate) as Investigated by Dielectric Spectroscopy

Ning Hao, Martin Böhning, Harald Goering, and Andreas Schönhals*

Federal Institute for Materials Research and Testing (BAM), Unter den Eichen 87, D-12200 Berlin, Germany

Received January 5, 2007; Revised Manuscript Received February 10, 2007

ABSTRACT: Nanocomposites were prepared by solution blending of polyhedral oligomeric silsesquioxane with phenethyl substituents (PhenethylPOSS) into poly(bisphenol A carbonate) (PBAC). The nanocomposites were investigated by dielectric spectroscopy, differential scanning calorimetry (DSC) and density measurements. PhenethylPOSS shows one relaxation process, the α-relaxation, confirmed by DSC investigations. PBAC shows a β-relaxation at lower and an α-relaxation at higher temperatures. With increasing PhenethylPOSS content the α-relaxation of the composites shifts to lower temperatures. Thus, incorporation of PhenethylPOSS leads to a plasticization of PBAC due to a decrease of the packing density which is rationalized by density measurements. For higher concentrations of PhenethylPOSS (>10 wt %) the α-relaxation of the polycarbonate matrix splits into two peaks. Moreover, close to the α-relaxation of PhenethylPOSS a third process is observed. These results indicate a phase separation into a PBAC matrix with a few percents of molecularly solved POSS and POSS-rich domains. These POSS-rich domains are surrounded by an interfacial layer of PBAC having a higher concentration of POSS than the matrix. A phase diagram is deduced providing a miscibility criterion. For the phase separated nanocomposites an interfacial polarization phenomena is observed. Using a simplified model the time constant of this process is correlated with the size of the PhenethylPOSS-rich domains and theire increasing size with the increase of the concentration of POSS.

1. Introduction

Polymer based nanocomposites continue to receive tremendous attention for various applications in conventional engineering but more and more also in the fields of microelectronics, organic batteries, optics, catalysis, etc. due to their favorable and often unique combination of properties (see, for instance, refs 2−11). Related to the small size of the filler particles, they show remarkable property improvements such as increased tensile properties, decreased gas permeability, decreased solvent uptake, increased thermal stability and flame retardance when compared to conventionally scaled composites. For designing new materials with desirable, predicted properties, a detailed understanding of the structure property relationships of nanocomposites is necessary. Although there is a large body of literature up to now, there is only a little knowledge about the relationship between the properties of the incorporated nanoparticles (shape, surface properties etc.) and the resulting morphology of the nanocomposite as well as its macroscopic behavior.

In particular, the role of the interface area between the nanoparticles and the polymer matrix is hardly discussed in the literature. Because of the high surface to volume ratio of the nanoparticles, the volume fraction of this interface area is high.[2,3,6] It is directly influenced by an adjacent nanoparticle surface and can play a decisive role for the performance of the nanocomposite material. For filler particles in the nanometer range the length scale of the interaction corresponds to the size of several segmental units of the host polymer. This means at first that the length-scale of interaction between filler particle and polymeric matrix is smaller than in conventional composite materials. Second, modifications in packing structure and dynamics of the polymer segments in the interface area between nanoparticle and matrix are expected.[7,12,13,15] This results in subtle changes in the free volume distribution that can give rise to significant property changes for the whole composite.

Different nanofillers like silica or related particles (see, for instance, refs 4, 7, 8, 14), layered silicates (clays) (see, for instance, refs 2−4, 6, and 15), nanosized metal particles,[9] or carbon nanotubes (see, for instance, refs 10 and 11) have been used to synthesize polymer based nanocomposites. Recently, there has been a strong interest to develop and investigate nanocomposites based on polyhedral oligomeric silsesquioxane (POSS;[1] see for instance, refs 16−19). The general chemical structure of POSS is shown in Figure 1a.

POSS consists of an inorganic silica core having organic substituents R. The general formula is $(SiO_{1.5})_nR_n$[17] where n is the number of silicon atoms of the inner cage. Using conventional synthesis conditions products with a predominant fraction of $n = 8$ (T8 cage) are obtained. POSS can be regarded as the smallest possible silica particle surrounded by an organic surface.[16,17] The chemistry of POSS is quite flexible. Therefore, a wide variety of substituents R can be linked to the inorganic silica core. This includes also the introduction of functional units and/or groups which can be polymerized.[16,17] For that reason, the compatibility between a "POSS nanoparticle" and the polymeric matrix can be tuned.[16]

In order to form stable polymer/nanoparticle systems, different routes have been proposed. Blending of nanoparticles into polymer matrices is a simple and inexpensive way to obtain polymer based nanocomposites. This can be done either via a solution route or by melt mixing. Recently this method has been also applied to prepare POSS/polymer nanocomposites.[19−28] An improvement of the material properties of these nanocomposites,

* Corresponding author. Telephone: +49 30/8104-3384. Fax: +49 30/8104-1637. E-mail: Andreas.Schoenhals@bam.de.

10.1021/ma070036c CCC: $37.00
Published on Web 03/17/2007

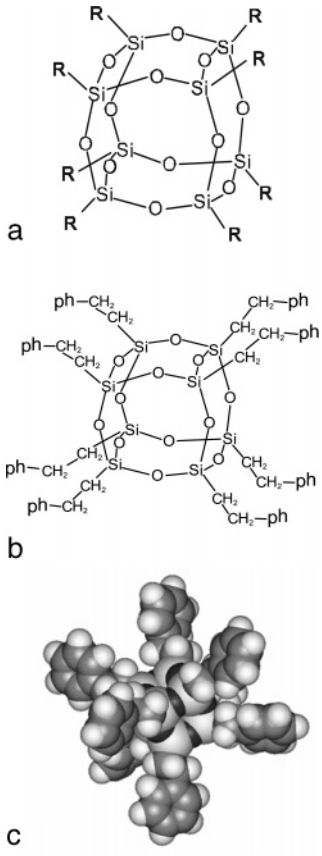

Figure 1. (a) General structure of a POSS molecule for the case of a T8 cage. (b) Chemical structure of octa-PhenethylPOSS (ph = phenyl). (c) octa-PhenethylPOSS as obtained by atomistic molecular modeling. The structure was minimized in vacuum with Insight II using the compass force field (Accelrys Inc.). In a second step a short MD simulation was carried out at $T = 308$ K for 10 ps using the same force field.

including the enhancement of the thermal stability and the mechanical properties, have been reported for different systems. For instance by incorporating trisilanol isooctyl POSS particles into poly(butylene terephthalate) (PBT) a more ductile composite product was obtained compared to the pure PBT.[22] Moreover it was also found that the glass transition temperature (T_g) of the nanocomposite depends on the substituents and the concentration of the POSS compound.

One critical feature of the blending method is the possible phase separation and agglomeration or even the crystallization of POSS during the preparation of the nanocomposite.[19] Transmission electron micrographs of polystyrene (PS) based nanocomposite presented by Blanski et al.[19,23] show that the solution compatibility of the POSS particles depends on the chemical nature of its side groups. An enhanced compatibility is expected when the POSS substituents and the matrix polymer contain similar groups or moieties.[19] However, this expectation is not fulfilled for all systems studied. According to recently published results of Kopesky et al., an aggregation of POSS is observed when the volume fraction of acrylic-POSS in poly(methyl methacrylate) (PMMA) is higher than 0.2.[24] The aggregates may have also impact on the material properties. By atomistic simulation Capaldi et al.[29] show that a possible phase separation is accompanied by a reduction of the volume fraction of the interfacial region. The properties of the material, which are correlated with the molecular mobility of the polymer matrix, depend on the geometry and size distribution of the POSS aggregates.

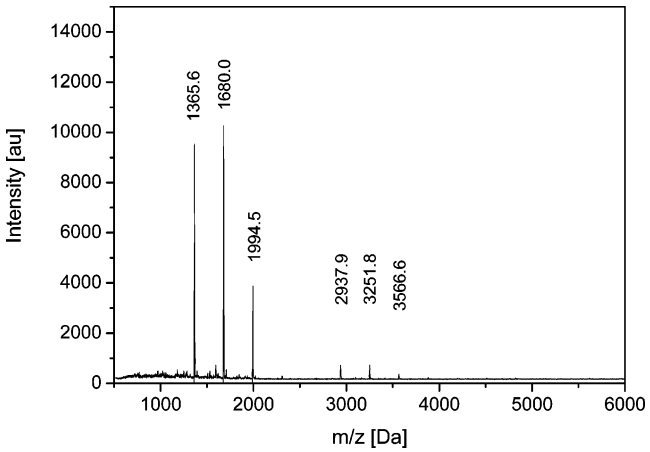

Figure 2. MALDI−TOF mass spectrum of PhenethylPOSS. The measurement was done by Bruker Reflex 3 spectrometer. As matrix nitrophenyl octyl ether with silver trifluoro acetate as salt is used. The mass difference of the peaks is 314 Da, which is equal to the mass of a $(SiO_{1.5})_2R_2$ unit where R is the phenethyl group.

In this contribution, nanocomposites based on poly(bisphenol A carbonate) (PBAC) and polyhedral oligomeric silsesquioxane with phenethyl substituents (PhenethylPOSS[1]) are prepared and investigated mainly by dielectric spectroscopy. PBAC is selected because of its remarkable mechanical properties. Moreover a lot of experimental work on PBAC itself but also on different nanocomposite materials based on it is already available in the literature (see, for instance, refs 28, 30, and 31). PhenethylPOSS has been chosen as nanofiller because of the phenyl groups in the substituents. Its chemical structure is outlined in Figure 1b. It is expected that the phenyl groups of the POSS molecule favorably interact with those of PBAC. Some results on POSS/PBAC nanocomposites using mechanical dynamical analysis have been reported recently.[28]

2. Experimental Section

2.1. Materials and Sample Preparation. PBAC was purchased from Sigma-Aldrich and used as matrix polymer ($M_n = 22000$ g/mol, PDI = 1.23). PhenethylPOSS was obtained from Hybrid-plastics, Inc.

To characterize the purchased PhenethylPOSS MALDI−TOF mass spectroscopy was carried out. Figure 2 gives the MALDI−TOF mass spectrum which shows well-defined peaks. The first peak corresponds to octa-PhenethylPOSS (T8). The difference in the masses of peaks is 314 Da. This difference corresponds exactly to $(SiO_{1.5})_2R_2$ where R is the phenethyl group. Therefore, it is concluded that the used product is a mixture of octa-PhenethylPOSS (T8), deca-PhenethylPOSS (T10), and smaller amounts of POSS of higher cage sizes. From the MALDI−TOF mass spectroscopy there is no indication for significant amounts of other ill-defined silsesquioxanes structures. Unfortunately, from the intensities of the peaks of the MALDI−TOF mass spectra no quantitative information about the fractions of the different cages can be obtained. However, it is known that for conventional synthesis conditions the major part of the product consists of T8 cages.[32,33] PhenethylPOSS is a viscous liquid at room temperature. Both materials were used without further purification.

To prepare the nanocomposites, in a first step, PBAC was dissolved in dichloromethane (DCM) with a concentration of 20 wt %. In a second step, PhenethylPOSS was solved with the selected concentrations in the PBAC/DCM solution. The mixture was then treated by ultrasonification (Bandelin Sonopuls, HD200/UW200 homogenizer equipped with KE76 titanium tapered tip) for at least 5 min and cast onto a polished glass substrate by a custom-made casting knife. During the casting the glass plate was placed in a closed chamber in order to control the initial evaporation of the

Table 1. Composition and Codes of the Investigated Nanocomposites and in Addition Its Glass Transition Temperatures Estimated by DSC and Its Densities

Sample Code	w_{POSS} [wt %]	T_g [K]	ρ [g/cm^3]
PhenethylPOSS	100	243.7	1.215
PC000	0	422.0	1.196
PC002	2.4	412.3	1.178
PC005	4.8	411.0	1.180
PC010	9.1	406.5	1.180
PC013	13.0	406.2	1.182
PC017	16.7	403.0	1.206
PC023	23.1	402.4	1.209
PC029	28.6	402.4	1.211
PC033	33.3	397.7	1.212
PC041	41.2	399.4	1.209

solvent from the prepared film. After this first evaporation step of the solvent, the films were depleted from the substrate. To remove the residual solvent the samples were dried in a second step in vacuum at 363 K for 24 h. The annealing temperature is below the glass transition temperature of polycarbonate. The presented procedure was selected because gas transport measurements were also carried out on the same set of samples. For these studies samples with relative large plane surfaces and without pinholes are required. Such samples cannot be obtained by annealing the film above its glass transition temperature. The results of the gas transport measurement will be published elsewhere[34] including a comparison with the dielectric data. The complete removal of the solvent was checked by thermogravimetric analysis (TGA). Moreover the glass transition temperature measured for a prepared, solvent caste pure polycarbonate film agrees with literature data given for bulk PBAC (see Table 1).

The thicknesses of the films vary between 50 and 100 μm. While the samples with low concentration of PhenethylPOSS are transparent those of higher concentrations are increasingly turbid. Details of the samples under investigation are listed in Table 1. The number in the sample codes corresponds to the nominal weight percentage of the incorporated PhenethylPOSS.

2.2. Methods. Broadband dielectric relaxation spectroscopy (BDRS) was applied to investigate the molecular mobility of the nanocomposites. This method is sensitive to molecular fluctuations of dipoles within the system. For polymers these fluctuations are related to the molecular mobility of groups, segments or the whole polymer chain as well. For details, see ref 35. The sample for the dielectric measurement is placed between two gold covered stainless steel electrodes in parallel geometry. The complex dielectric function $\epsilon^*(f) = \epsilon'(f) - i\epsilon''(f)$ (f = frequency, ϵ' and ϵ'' = real and imaginary part of the complex dielectric function, and $i = \sqrt{-1}$) is isothermally measured in the frequency range from 10^{-1} to 10^7 Hz by a high-resolution ALPHA analyzer (Novocontrol, Hundsangen, Germany). The temperature of the sample is controlled by a Quattro Novocontrol cryo-system with a temperature stability better than 0.1 K. For a detailed description of the used dielectric equipment see for instance.[36]

The thermal analysis was carried out by differential scanning calorimetry (DSC, Seiko instruments). N_2 is used as protection gas. The samples were measured in the temperature range from 173 to 473 K with a heating rate of 10 K/min. The glass transition temperature T_g was taken as the inflection point of the heat flow of the second heating run.

The density of the samples was measured according to DIN 53 479 by a density gradient column at the required temperature of 296.15 K (23 °C). The error in the temperature control was 0.3 K. To measure densities in the range from 1.175 to 1.220 g/cm^3 concentrated solutions of $Ca(NO_3)_2$ with distilled water were employed. The density of the sample is determined by polynomial interpolation between the densities of calibrated glass floats. The first value of the density is taken 1 day after the insertion of the sample into the density gradient. During 1 week each day a value of the density is taken and the average value is calculated. The error of these subsequent measurements is below 1%. The absolute error in the calibration of the glass floats is 1.97%. It should be noted that it is not the aim of the paper to give absolute values of density but to discuses its relative change with the increase of the concentration of PhenethylPOSS. Therefore, all samples are measured at same time using the same density gradient.

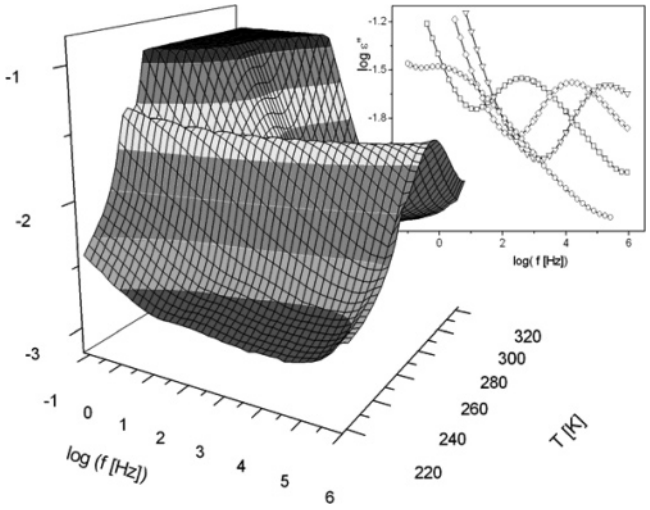

Figure 3. Dielectric loss vs frequency and temperature for pure PhenethylPOSS in 3D representation. The inset gives the dielectric loss vs frequency for pure PhenethylPOSS at different temperatures: (○) T = 247.2 K; (□) 257.2 K; (◇) 267.1 K; (▽) 277.1 K. The lines are guides to the eyes.

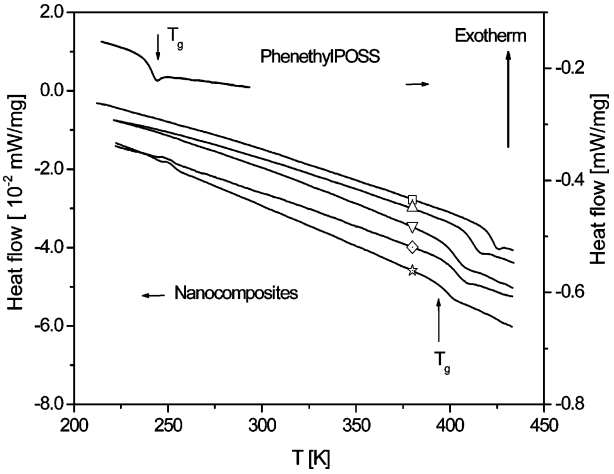

Figure 4. DSC measurements for PhenethylPOSS, PBAC and corresponding nanocomposites: (□) PBAC; (△) PC005; (▽) PC017; (◇) PC023; (☆) PC033. For clarity the heat flow traces of the nanocomposites are shifted in y-direction.

3. Results and Discussion

Figure 3 gives the dielectric loss of pure PhenethylPOSS vs frequency and temperature in a 3D-representation. One dielectrically active relaxation process indicated by a peak in ϵ'' is observed (see also inset Figure 3). It is assigned to the dynamic glass transition or α-relaxation of PhenethylPOSS. This interpretation is in agreement with corresponding DSC measurements, which show the characteristic step-like change in the heat flow (see Figure 4). The reason why the used PhenethylPOSS undergoes a glass transition is not clear at this time. Possibly, the different cages sizes present in the product prevent crystallization. A detailed discussion of the glass transition of PhenethylPOSS will be published separately.[37]

For PBAC the dielectric loss is given as a function of temperature at a fixed frequency of 10 kHz in Figure 5. At least

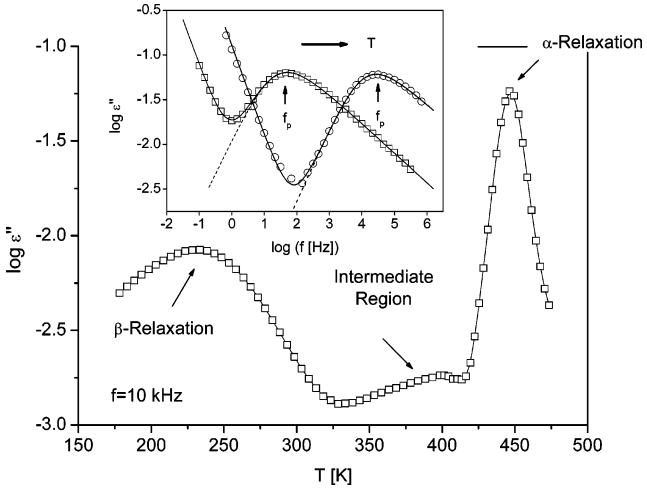

Figure 5. Dielectric loss vs temperature for pure PBAC at a frequency of 10 kHz. The line is a guide for the eyes. The inset gives the dielectric loss vs frequency for two different temperatures above T_g: (□) 433.2 K; (○) 448.6 K. The solid line is a fit of the HN-function to the data including a conductivity contribution. The dashed line gives the contribution of the relaxation process.

two relaxation regions indicated by peaks in ϵ'' could be identified. The β-relaxation at low temperatures is assigned to localized fluctuations. There is evidence from NMR and neutron scattering experiments that the β-process in PBAC should be related to fluctuations of the phenyl ring (see, for instance, ref 38). For the carbonyl group, being the only polar structure in the repeat unit of PBAC, it has to be also involved in the β-relaxation in order to be dielectrically visible.[39−41] At higher temperatures than the β-process, the α-relaxation (dynamic glass transition) takes place. This relaxation process is related to cooperative segmental fluctuations of PBAC. In the temperature range between the β- and α-relaxation, a third complex process can be identified. This region is called "intermediate relaxation region".[30,42] Its molecular assignment is still under discussion in the literature.

The dielectric measurements are analyzed by fitting the model function of Havriliak−Negami (HN-function)[43] to the data which reads

$$\epsilon^*(f) - \epsilon_\infty = \frac{\Delta\epsilon}{\left(1 + \left(\frac{if}{f_0}\right)^\beta\right)^\gamma} \qquad (1)$$

f_0 is a characteristic frequency related to the frequency of maximal loss f_p (relaxation rate), ϵ_∞ describes the value of the real part ϵ' for $f \gg f_0$. β and γ are fractional parameters ($0 < \beta \le 1$ and $0 < \beta\gamma \le 1$) characterizing the shape of the relaxation time spectra. $\Delta\epsilon$ denotes the dielectric strength. Conduction effects are treated in the usual way by adding a contribution $\sigma_0/[(2\pi f)^s\epsilon_o]$ to the dielectric loss where σ_0 is related to the specific DC conductivity of the sample and ϵ_0 is the dielectric permittivity of vacuum. The parameter s ($0 < s \le 1$) describes for $s = 1$ Ohmic and for $s < 1$ non-Ohmic effects in the conductivity. For details, see ref 44.

The inset of Figure 5 gives some examples of fitting the HN equation to the α-relaxation of PBAC. In Figure 6 the relaxation rates f_p for the pure components are plotted vs reciprocal temperature. The temperature dependence of the relaxation rate f_p of the α-relaxation of both, PBAC and PhenethylPOSS, can

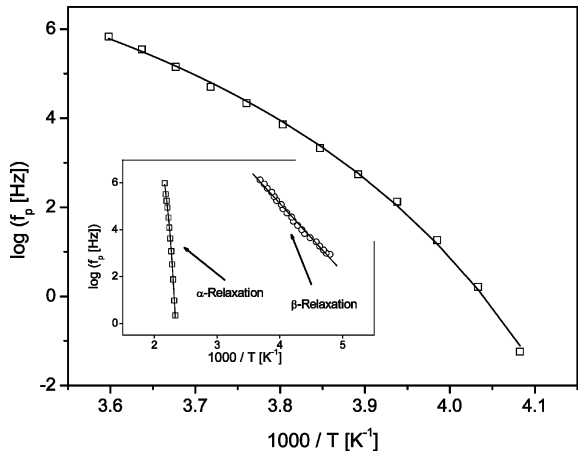

Figure 6. Relaxation rate f_p vs inverse temperature for PhenethylPOSS. The line is a fit of the VFT equation (eq 2) to the data. The inset gives the same for PBAC: (□) α- and (○) β-relaxation. The lines are fits of the VFT-equation to the data of the α-relaxation and the Arrhenius equation to that of the β-process. For the parameters, see Table 2.

Table 2. Estimated VFT Parameters for the α-Process and Activation Parameters for the β-Process

	α-relaxation			β-relaxation	
sample code	log(f_∞ [Hz])	A [K]	T_0 [K]	E_A [kJ/mol]	log(f_∞ [Hz])
PhenethylPOSS	11.4	334	218.2		
PC000	13.7	611.3	382.6	59.5	16.8
PC002	11.6	437.7	382.8	57.6	15.5
PC005	11.0	386.7	383.0	53.2	16.1
PC010	10.4	311.8	386.1	54.4	16.8
PC013	11.3	422.8	374.6	50.6	16.0
PC017	9.3	236.4	386.0	47.8	14.7
PC023	10.7	245.9	399.9	46.3	13.7
PC029	10.8	246.1	398.6	48.9	16.1
PC033	9.4	182.6	398.6	49.7	15.4
PC041	10.6	311.1	384.8	48.5	16.2

be well described by the Vogel−Fulcher−Tammann (VFT) equation[45] which reads

$$\log f_p = \log f_\infty - \frac{A}{T - T_0} \qquad (2)$$

(log f_∞, A = constants; T_0 is the so-called Vogel temperature). For the β-relaxation of PBAC, the data follow the Arrhenius law

$$f_p = f_\infty \exp\left(-\frac{E_A}{k_B T}\right) \qquad (3)$$

(E_A = activation energy, f_∞ = pre-exponential factor, and k_B = Boltzmann's constant). All fit parameters are given in Table 2.

Depending on the concentration of PhenethylPOSS, the dielectric spectra of the nanocomposites show a variety of dielectrically active phenomena like an α- and a β-relaxation. In addition to that, a special kind of an interfacial polarization process[44] is observed which is caused by blocking of charge carriers at internal phase boundaries. In the following sections the dielectric processes of the nanocomposites are discussed separately in their dependence on the concentration of PhenethylPOSS together with the resulting complex phase behavior of the nanocomposite materials. The dynamic glass transition (α-relaxation) is addressed first, followed by an analysis of the β-relaxation. Finally the interfacial polarization process is analyzed in detail in the context of a phase separation model.

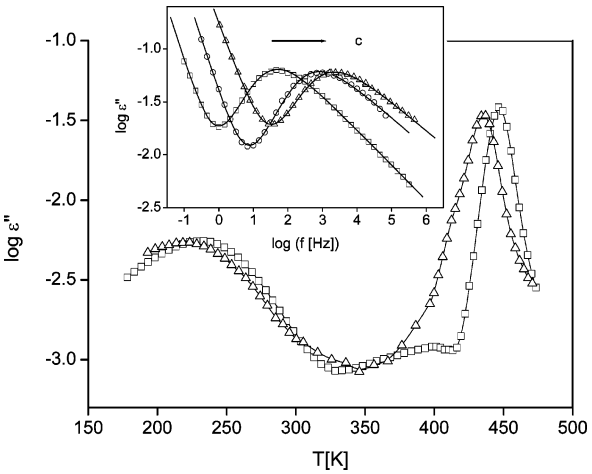

Figure 7. Dielectric loss vs temperature for pure PBAC (□) and PC005 (△) at a frequency of 10 kHz. The lines are guides for the eyes. The inset gives the dielectric loss vs frequency for different nanocomposites at a temperature of $T = 433.15$ K: (□) PBAC; (○) PC002; (△) PC005. The lines are fits of the HN-function to the data including a conductivity contribution.

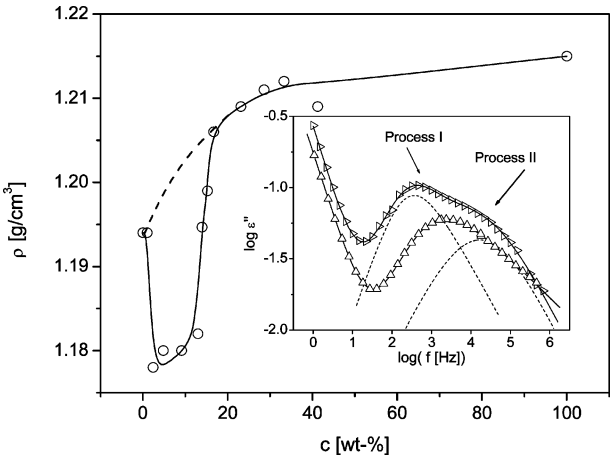

Figure 8. Density of the nanocomposites vs concentration. The value of the pure PhenethylPOSS is a lower estimate. The dashed line may roughly characterize an additive behavior. The inset gives the dielectric loss vs frequency for different nanocomposites at a temperature of $T = 433.15$ K: (△) PC005; (triangle pointing right) PC010. The lines are fits of one (PC005) or two (PC010) HN-functions to the data including a conductivity contribution. The dashed lines represent of the two relaxational contributions for PC010.

Dynamic Glass Transition (α-Relaxation). Figure 7 compares the dielectric loss of a PhenethylPOSS/PBAC nanocomposite with a low concentration of POSS (ca. 4.8 wt %, sample PC005) with that of pure polycarbonate. For the composite also a β- and an α-relaxation is observed. Compared to pure PBAC, both relaxation processes are shifted to lower temperatures.

The inset of Figure 7 gives the dielectric loss spectra of different nanocomposites at the same temperature above the glass transition temperature ($T = 433.15$ K). Only one single relaxation process is observed which indicates that PhenethylPOSS is miscible within the PBAC matrix on a molecular level for the considered concentrations of 2.4 and 4.8 wt %. With increasing concentration of POSS the dielectric loss peak shifts to higher frequencies in agreement with the corresponding DSC measurements (see Figure 4). This increase in molecular mobility (or decreased glass transition temperature) is known as plasticization. A similar behavior is discussed in refs 24 and 25 for nanocomposites prepared from PMMA and different POSS compounds with acrylic, cyclohexyl, and isobutyl substituents.

The mechanism of the plasticization of the polymer matrix by PhenethylPOSS is quite different from that caused by low molecular weight molecules (conventional plasticizers). Because of the phenethyl groups (or large substituents in general) PhenethylPOSS is a quite bulky molecule. Figure 1c gives its structure as obtained by atomistic molecular modeling. For modeling details see the figure caption. For steric reasons and due to the short spacers ($-CH_2-CH_2-$ groups), the planes of the phenyl rings cannot be arranged in parallel to the silica core, which would correspond to the theoretically densest packing. Because of the short spacer, the volume of this structure is more or less fixed and the substituents of the molecules are expected to be more or less immobile. When the PhenethylPOSS molecule is incorporated in a polymer matrix, it is assumed that the discussed arrangement of the phenyl rings is probably not changed. So the packing density of the surrounding matrix is decreased which results in a local increase of the free volume. This line of argumentation is supported by density measurements (see Figure 8). For low concentrations of PhenethylPOSS the density of the nanocomposites is strongly reduced compared to that of pure PBAC.

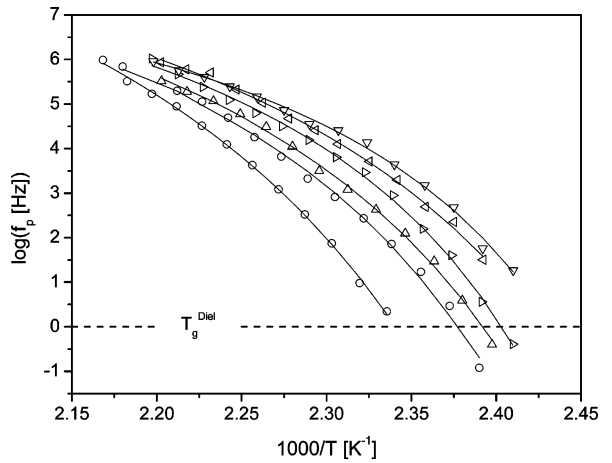

Figure 9. Relaxation rate f_p vs inverse temperature for the nanocomposites with low concentrations of PhenethylPOSS: (□) PBAC; (○) PC002; (△) PC005; (triangle pointing right) PC010; (triangle pointing left) PC013; (▽) PC017. Lines are fits of the VFT equation to the data. The dashed line symbolizes the relaxation rate where T_g^{Diel} is taken.

In Figure 9, the relaxation rates f_p for the composites with low concentrations of PhenethylPOSS are plotted vs reciprocal temperature. As expected from the raw data the curves shift to lower temperatures with increasing concentration of PhenethylPOSS. By fitting the VFT equation to the data a dielectric glass transition temperature $T_g^{Diel} = T(f_p = 1\ \text{Hz})$ can be estimated. The VFT parameters are summarized in Table 2.

In the inset of Figure 8, the frequency dependence of the dielectric loss of two nanocomposites, one having a lower and one having a higher concentration of PhenethylPOSS, is compared at the same temperature. For the nanocomposite with the higher concentration (10 wt %) of POSS a double peak structure can be observed in the dielectric loss. Unfortunately, due to the strong overlap of these two processes they cannot be analyzed separately without uncertainty. An overview over the whole dielectric behavior of a PBAC/PhenethylPOSS nanocomposite with a higher concentration of POSS gives Figure 10 where the dielectric loss is plotted vs temperature for pure PBAC, pure PhenethylPOSS and a nanocomposite with 28.6 wt % PhenethylPOSS (PC029). For the nanocomposite,

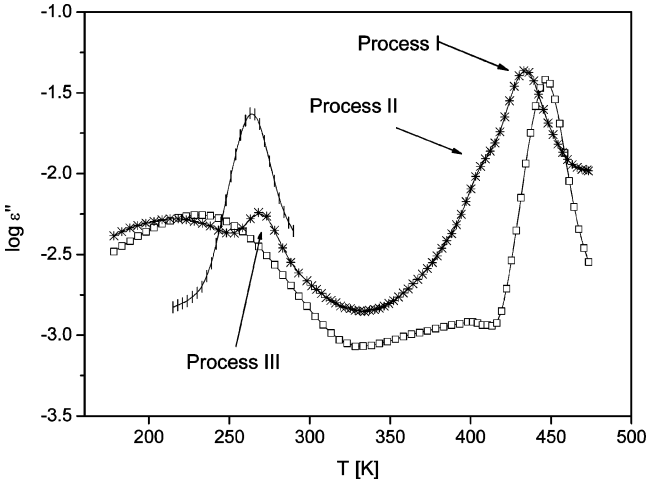

Figure 10. Dielectric loss vs temperature at a frequency of 10 kHz for pure PBAC (□) and PC029 (∗) in comparison with that of pure PhenethylPOSS (|). The lines are guides for the eyes.

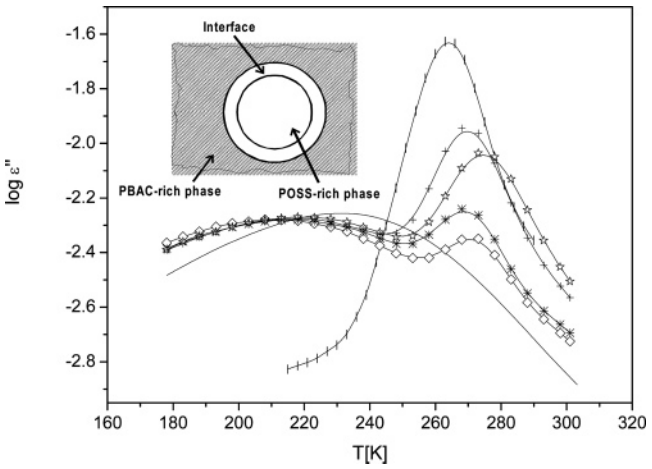

Figure 11. Dielectric loss vs temperature at a fixed frequency of 10 kHz in the temperature range of the glass transition temperature of PhenethylPOSS for different concentrations of PhenethylPOSS: (—) β-relaxation PBAC; (◇) PC023; (∗) PC029; (☆) PC033; (+) PC041; (|) PhenethylPOSS. Lines are guides for the eyes. The inset gives a scheme of the proposed phase structure.

in the region of the α-relaxation of PBAC again a double peak structure (processes I and II in Figure 10) is observed as already discussed for the isothermal data. In parallel, in the temperature region of the glass transition of pure PhenethylPOSS a third relaxation process is evident, indicated by an additional peak in ϵ'' (process III in Figure 10). The appearance of multiple peaks in the dielectric spectra has to be assigned to phase separation which take place in nanocomposites with higher concentrations of PhenethylPOSS. In the following, the assignment of the different processes is discussed in detail.

The interpretation of processes III and I is straightforward. According to the considerations for nanocomposites with a low concentration of POSS process I has to be assigned to the glass transition of the PBAC-rich matrix. Because the glass transition temperature is reduced compared to bulk polycarbonate it is concluded that PhenethylPOSS is dispersed in this matrix on a molecular level to a few present (see below). Process III is observed close to the glass transition of PhenethylPOSS. Its dielectric intensity increases with increasing concentration of PhenethylPOSS. (see Figure 11). Obviously this process has to be related to the α-relaxation of PhenethylPOSS-rich domains.

Process II is located close to process I. Therefore, it is concluded that this process is related mainly to polycarbonate.

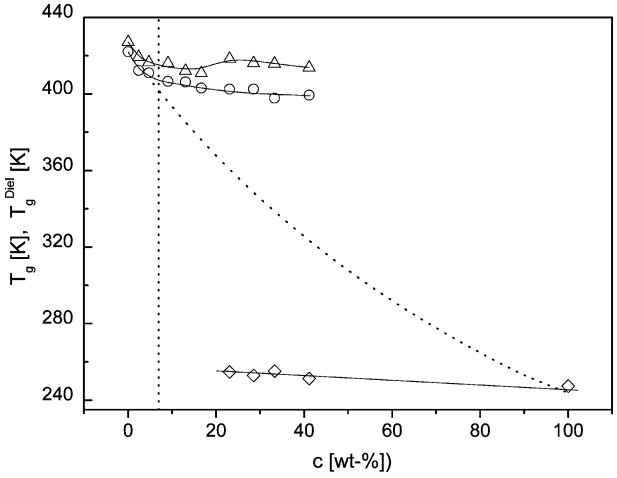

Figure 12. Dependence of the thermal glass transition temperature T_g (○) and the dielectric glass transition temperature T_g^{Diel} (□) for the PBAC-rich phase on the concentration of PhenethylPOSS. ◇ gives the dielectric glass transition temperature of the POSS-rich domains. Solid lines are guides for the eyes. The dotted line is the expectation from the Fox-equation. The dashed line indicates the miscibility limit.

But its relaxation rate is lower than that of process I. This means that more PhenethylPOSS molecules are involved in process II than in process I. According to the Gibbs phase rule the number of possible phases at constant pressure and temperature is two. Therefore, process II is assigned to an interfacial layer between the POSS-rich domains and the PBAC-rich phase. A sketch of the proposed phase structure is given in the inset of Figure 11. To have a signature in the dielectric spectra the interfacial layer should have a certain spatial extent. To allow the observed glassy dynamics the characteristic size of this interphase is expected to be in the range between 1 and 3 nm.[12,46,47]

From the relaxation experiments, one can conclude that for higher concentrations of PhenethylPOSS the nanocomposites have a two phase structure consisting of a PBAC-rich phase and a POSS-rich phase. Both phases are separated by an interfacial layer. The discussed change in the phase behavior is also reflected by the dependence of the density of the nanocomposites on the concentration of POSS. The density is an overall bulk property of the whole sample. For low concentrations of PhenethylPOSS—in the non-phase separated state—the observed decrease in the density is due to an increase of free volume between POSS particles and the PBAC segments. For concentrations greater than 10 wt %, this increase of free volume is overcompensated by the formation of the POSS-rich domains having approximately the same density as PhenethylPOSS itself. Therefore, the density strongly increases and approaches a line which may be roughly expected for a simple two phase system (see Figure 8).

The relaxation behavior of the nanocomposites as seen by investigating the dynamic glass transition can be summarized by constructing a phase diagram. In Figure 12 the thermal glass transition temperature T_g, and the dielectric glass transition temperature T_g^{Diel} is plotted vs concentration of PhenethylPOSS. In addition the prediction from the Fox equation

$$\frac{1}{T_g} = \frac{c_{PBAC}}{T_{gPBAC}} + \frac{c_{POSS}}{T_{gPOSS}} \quad (c_{PBAC} + c_{POSS} = 1) \qquad (4)$$

is given which is expected to be valid for a molecularly miscible system. Up to a concentration of 5 wt % the data follow the Fox equation. So it is concluded that up to this concentration

PhenethylPOSS can be dispersed on a molecular level in PBAC. This is in agreement with the observation that for a nanocomposite with 5 wt % PhenethylPOSS only one peak is observed in the temperature range of the dynamic glass transition (see inset Figure 8). For 10 wt % and higher concentrations of PhenethylPOSS the thermal glass transition temperature T_g shows a much weaker dependence on concentration than predicted by the Fox-equation. This indicates a strongly reduced miscibility of PhenethylPOSS in PBAC. This dependence levels off for high concentrations of PhenethylPOSS. For these concentrations PhenethylPOSS can no longer completely dissolved into PBAC on a molecular level. In parallel, as already stated, a double peak in dynamic glass transition is observed. Therefore, it is concluded that the maximum concentration for a molecular miscibility of PhenethylPOSS into PBAC is between 5 and 10 wt % at ca. 7 wt % PhenethylPOSS.

The concentration dependence of the dielectric glass transition temperature T_g^{Diel} is a bit more complex. The inset of Figure 8 shows that the α-relaxation peak splits into two components. The low-frequency process for 10 wt % of PhenethylPOSS is shifted to lower frequencies in comparison to the loss peak of the nanocomposite of 5 wt %. This corresponds to a slight (relative) increase of the dielectric glass transition temperature as seen in Figure 12, which indicates the formation of a PBAC-rich phase and the interfacial layer. It has to be noted that this fine structure of the loss peak cannot be resolved by the thermal measurements by DSC (see Figure 4). In future additional measurements are planed like temperature modulated DSC experiments.

The dielectric glass transition temperature of the POSS-rich domains increases with decreasing content of PhenethylPOSS (see Figure 12). Since PBAC has an essentially higher glass transition temperature than PhenethylPOSS it is concluded that also some PBAC is present in these domains.

***β*-Relaxation.** In the following the dependence of the β-relaxation on the concentration of PhenethylPOSS will be discussed. Figure 7 shows that the β-process is shifted to lower temperatures for the nanocomposites compared to pure PBAC. This indicates also an enhancement of the localized molecular mobility in addition to the segmental mobility. In general, when a glassy polymer is plasticized by a low molecular weight plasticizer the α-process shifts to lower temperatures. However, in parallel, the β-relaxation shifts in the opposite direction to higher temperatures. This phenomenon is called antiplasticization.[48,49] But here, for the investigated nanocomposite material both relaxation processes shifts in the same direction to lower temperatures. This result also supports the conclusion that the plasticization of the PBAC matrix by PhenethylPOSS is different from that caused by a conventional low molecular weight plasticizer.

The temperature dependence of the relaxation rates follows the Arrhenius equation and the activation energy E_A is estimated by fitting of eq 3 to the data. In Figure 13, E_A is plotted vs the concentration of PhenethylPOSS. Up to 10 wt % the activation energy decreases with increasing concentration of PhenethylPOSS. As is the case for the α-relaxation, the reduced packing density of the matrix leads to an increase of the free volume. This enhances, in addition to the cooperative segmental dynamics, also the mobility of localized fluctuations observed as decrease of their activation energy.

For concentrations of PhenethylPOSS higher than 10 wt % the value of the activation energy remains constant. This is in full agreement with the results obtained by analyzing the dynamic glass transition which gave the result that

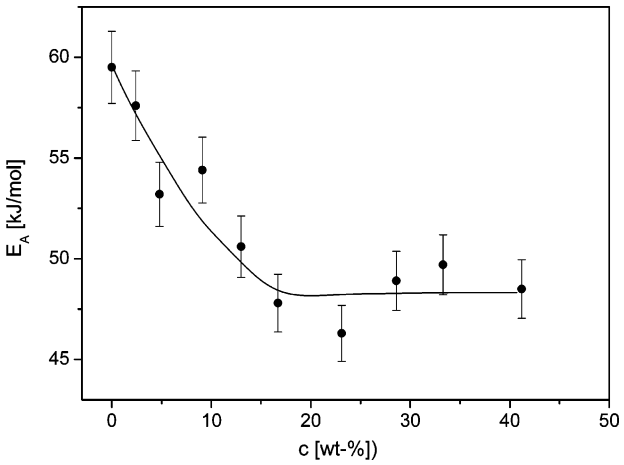

Figure 13. Activation energy E_A of the β-relaxation vs the concentration of PhenethylPOSS. The line is a guide for the eyes.

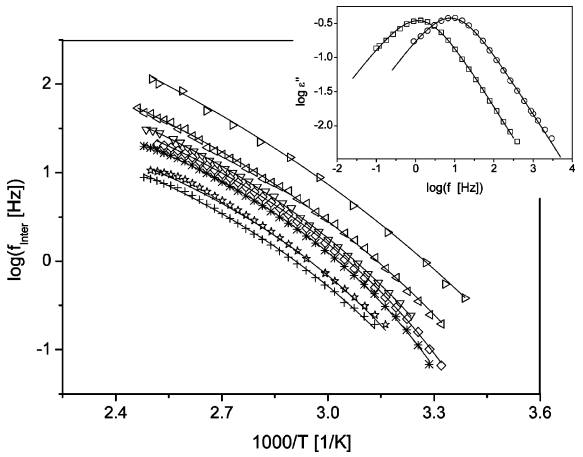

Figure 14. Characteristic frequencies f_{Inter} of the interfacial polarization vs inverse temperature: (triangle pointing right) - PC010; (triangle pointing left) - PC013; ▽- PC017; ∗- PC029; ◇ - PC023; ☆ - PC033; + - PC041. The lines are guides for the eyes. The inset gives the dielectric loss vs frequency of the interfacial polarization for PC033 at temperatures below the glass transition temperature of the PBAC-rich matrix (T_g = 397.7 K, see Table 1): □ - 343.1 K; ○ - 388.1 K. The lines are fits of the HN-function to the data.

PhenethylPOSS can be molecularly dispersed up to 7 wt % into PBAC.

Interfacial Polarization. For the nanocomposites with higher concentrations of PhenethylPOSS a pronounced peak in the dielectric loss at low frequencies is observed at temperatures lower than the glass transition temperature of the PBAC-rich matrix (see inset Figure 14). In comparison with the α-relaxation the width of the peak is much smaller, its shape is more symmetric (compare to inset Figure 7) and its intensity is high. As discussed below, this process is assigned to a special kind of interfacial polarization process due to the blocking of charge carriers at internal phase boundaries.

Generally such an interfacial polarization process is caused by blocking of charge carriers at internal surfaces or interfaces of different phases having different values of the dielectric permittivity and/or conductivity. An example for such a process is at mesoscopic length scales the Maxwell−Wagner−Sillars (MWS) or at macroscopic length scales the electrode polarization (for details, see ref 44). Normally for polymer based composites such a process is observed at higher temperatures than the glass transition temperature of the matrix. This is due

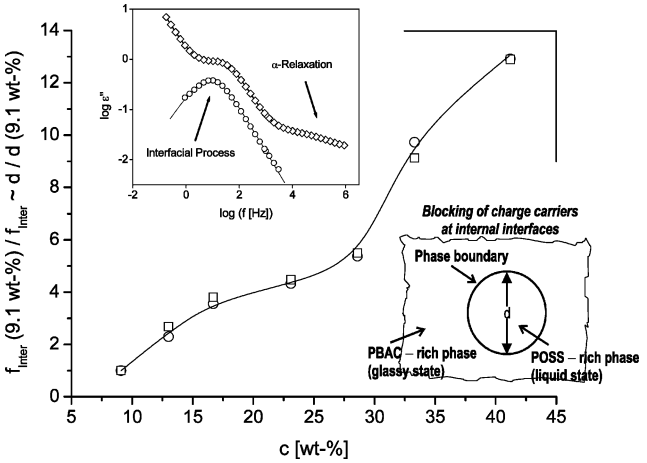

Figure 15. Dependence of the characteristic rate of the interfacial polarization vs concentration of PhenethylPOSS reduced by the rate of the sample with 9.1 wt % PhenethylPOSS for two different temperatures: □ - 370.3 K; ○ - 333.3 K. The line is a guide for the eyes. For details see eq 6. The inset gives the dielectric loss vs frequency of the interfacial polarization for PC033 at temperatures below and above the glass transition temperature of the PBAC-rich matrix (T_g = 397.7 K, see Table 1) □ - 343.1 K and above ○ - 433.1 K. The lines are guides for the eyes. The scheme presents the model for the interfacial polarization.

to the fact that in most cases inorganic nanoparticles like clays etc. are dispersed in a polymeric matrix. The mobility of charge carriers is related to the segmental dynamics which sets in above T_g. Therefore, charge carriers become mobile above T_g and their blocking at the organic/inorganic interface causes an interfacial polarization process above T_g.

Here in the considered case, an interfacial polarization process is observed at temperatures lower than T_g characterizing the nanocomposite as a whole. To understand this, one has to keep in mind that for higher concentrations of PhenethylPOSS the nanocomposite has a phase separated structure with POSS-rich domains. The glass transition temperature of these domains is essentially lower than that of the PBAC-rich phase. Therefore, the charge carriers inside these domains have even below $T_{g,PBAC-rich}$ a higher mobility and can be driven by an electrical field. But their movement is blocked at the interfaces to the PBAC-rich phase which still is in the glassy state. This causes an interface polarization process at temperatures below $T_{g,\ PBAC-rich.}$ related to the POSS-rich domains (see scheme in Figure 15).

Although an interfacial polarization is not a relaxation process it can be also analyzed by fitting the HN-function to the data (see inset Figure 14). In Figure 14 the characteristic rates of the interfacial polarization process are plotted vs reciprocal temperature. At a fixed temperature the rate of the interfacial polarization decreases with increasing PhenethylPOSS concentration. This result reflects the fact that with increasing concentration of PhenethylPOSS the size of the POSS-rich domains become larger and in average the charge carriers need a longer time to diffuse through it before being blocked at the internal phase boundary. This can be quantitatively discussed in an oversimplified model. In the direction of the electrical field the POSS-rich domains are described as a mobile layer of thickness d between solid walls representing the surrounding glassy PBAC-rich phase. d roughly characterizes the size of the probably spherical POSS-rich domains. The blocking of the charge carriers at these walls is described by an electrical double layer with an effective spacing characterized by its Debye length L_D. This double layer represents an additional capacitance C_{DL} in the system and the time dependence of the polarization is due to charging/discharging of that electrical double layer. The time constant τ_{Inter} for this process can be estimated in the simplest possible approach analogous to that for electrode polarization[44] and is related to the conductivity σ of the domains. Considering the conductivity to be inversely proportional to the domain size $\sigma \sim (\sigma_0/d)$, one obtains

$$\tau_{Inter} = \frac{C_{DL}}{\sigma} \approx \frac{\epsilon_S \epsilon_0}{\sigma_0} \frac{d}{2L_D} \tag{5}$$

ϵ_0 is the dielectric permittivity of vacuum, ϵ_S is the permittivity and σ_0 is the specific dc-conductivity within the POSS-rich domain. Assuming further that ϵ_S, σ_0, and L_D depend only weakly on the overall POSS concentration the relative change of the mean size of the POSS-rich domains can be estimated by

$$\frac{\tau_{Inter,1}}{\tau_{Inter,2}} = \frac{f_{Inter,2}}{f_{Inter,1}} \approx \frac{d_1}{d_2} \tag{6}$$

from the data shown in Figure 14. A similar approach was discussed in ref 15 for silicate layers dispersed in a modified polypropylene matrix. In Figure 15, the change of the characteristic rate of the interface polarization is plotted vs the concentration of PhenethylPOSS for two different temperatures. As expected from the model consideration, there is no significant temperature dependence because the PBAC-rich matrix is always in the glassy state. With increasing concentration of PhenethylPOSS the size of the domains increases as expected. For medium concentrations (15−25 wt %) this change is quite moderate (see Figure 15). This can be discussed in the following model. For low and medium concentration of PhenethylPOSS first the number of POSS-rich domains increases with increasing concentration of POSS rather than their size. This causes the plateau-like change of the domain size in the concentration range between 15 and 25 wt %. For higher concentrations of PhenethylPOSS the size of the domains increases strongly up to about 13 times (41.2 wt %) compared to the size of the domains formed for about 10 wt % PhenethylPOSS.

The simple model discussed above is based on the assumption that the PBAC-rich phase is in the glassy state. Therefore, changes in the temperature dependence of the interfacial polarization are expected when the temperature is increased to values above the glass transition temperature of the PBAC-rich phase ($T_{g,PBAC-rich}$). The inset of Figure 15 compares the interfacial polarization spectra of the sample PC033 for temperatures below and above $T_{g,PBAC-rich}$. Pronounced differences are obvious already in these raw data. Figure 16 analyses the temperature dependence of the characteristic rate (f_{Inter}) and of the dielectric strength ($\Delta\epsilon_{Inter}$) of the interfacial polarization for the sample PC033. Both quantities show a drastic change in its temperature dependence at $T_{g,PBAC-rich.}$ For f_{Inter} the temperature dependence above $T_{g,\ PBAC-rich}$ is distinctly weaker than below it, while the dielectric strength of the interfacial polarization process increases strongly above $T_{g,PBAC-rich.}$ These results support the model discussed above. For a more quantitative discussion further experiments and more detailed model considerations are necessary.

Conclusion

Nanocomposites were prepared by blending polyhedral oligomeric silsesquioxane with phenethyl substituents into poly(bisphenol A carbonate) matrices by a well adapted solution

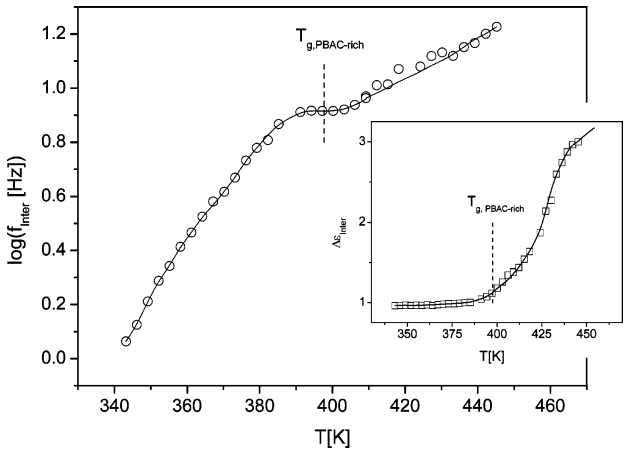

Figure 16. Characteristic frequencies f_{Inter} of the interfacial polarization vs temperature for PC033 below and above the thermal glass transition $T_{g,PBAC-rich}$. The inset gives the same for the dielectric strength of the interfacial polarization $\Delta\epsilon_{Inter}$. Lines are guides for the eyes.

casting method. The evaporation of the solvent was controlled by adjusting the vapor pressure of the solvent in a closed chamber. As a result homogeneous and almost transparent films are obtained by this procedure for a reasonable concentration range of PhenethylPOSS from 0 to 40 wt %.

Dielectric spectroscopy shows that for low concentrations of PhenethylPOSS ($\leq$10 wt %) the dynamic glass transition of the PBAC matrix is shifted to lower temperatures with increasing PhenethylPOSS content. DSC investigations gave the same result. This means at this concentrations level PhenethylPOSS acts as a plasticizer. But in contrast to low molecular weight plasticizers this is clearly due to a decrease of the molecular packing (increase of free volume) which is experimentally confirmed by density measurements.

For higher concentrations of PhenethylPOSS ($\geq$10 wt %) the dielectric spectra show a double peak structure. The two corresponding relaxation processes are assigned to the dynamic glass transitions of a PBAC-rich phase and an interfacial layer having different concentrations of PhenethylPOSS. In parallel at temperatures close to the glass transition temperature of PhenethylPOSS a third peak is observed with an intensity increasing with the concentration of PhenethylPOSS. This relaxation process is assigned to the dynamic glass transition of PhenethylPOSS-rich domains. With increasing PhenethylPOSS content this relaxation process shifts to lower temperatures. This phase separation is also reflected in the temperature dependence of the density of the nanocomposites.

From the DSC measurements and in more detail from the dielectric studies a phase diagram for the PhenethylPOSS/PBAC nanocomposites is deduced. This phase diagram shows that PhenethylPOSS is miscible in PBAC on a molecular level up to about 7 wt %. Approximately the same concentration limit for the molecular miscibility of PhenethylPOSS into PBAC is obtained by a quantitative analysis of the β-relaxation of PBAC. Its activation energy decreases up to 10 wt % of dispersed PhenethylPOSS and remains constant at this level for higher concentrations of the used POSS filler.

For the phase separated nanocomposites, in addition to the relaxation processes an interphase polarization process is observed which is due to blocking of charge carriers at internal phase boundaries. Using a simple model a characteristic size of the POSS-rich domains and its relative growth with increasing concentration of PhenethylPOSS can be estimated by analyzing the time constant of this polarization process.

Acknowledgment. The authors gratefully acknowledge the assistance of our colleagues O. Hölck and D. Neubert for there experimental help as well as Dr. M. Heuchel (GKSS Research Centre) for the molecular model of PhenethylPOSS. Dr. R. P. Krüger (BAM) is thanked for caring out the MALDI−TOF mass spectroscopy measurements. The financial support from the Ph.D. program of BAM (to N.H.) is highly appreciated.

References and Notes

(1) POSS and PhenethylPOSS are trade marks for polyhedral oligomeric silsesquioxane and phenethylsilsesquioxane (MS0870) of Hybrid Plastics Inc. (Hattiesburg, MS), respectively. See also www.hybrid-plastics.com.
(2) Novak, B. M. *Adv. Mater.* **1993**, *5*, 422.
(3) Krishnamoorti, R.; Vaia, R. A. *Polymer Nanocomposites*; ACS Symposium Series 804; Amercian Chemical Society: Washington, DC, 2002.
(4) Mackay, M. E.; Dao, T. T.; Tuteja, A.; Ho, D. L.; Van Horn, B.; Kim, H. C.; Hawker, C. J. *Nat. Mater.* **2003**, *2*, 762.
(5) Schmidt, G.; Malwitz, M. M. *Curr. Opin. Colloid Interface Sci.* **2003**, *8*, 103.
(6) Vaia, R. A.; Giannelis, E. P. *MRS Bull.* **2001**, *26*, 394.
(7) Davis, S. R.; Brough, A. R.; Atkinson, A. *J. Non-Cryst. Solids* **2003**, *315*, 197.
(8) Merkel, T. C.; Freeman, B. D.; Spontak, R. J.; He, Z.; Pinnau, I.; Meakin, P.; Hill, A. J. *Science* **2002**, *296*, 519. Merkel, T. C.; He, Z.; Pinnau, I.; Freeman, B. D.; Meakin, P.; Hill, A. J. *Macromolecules* **2003**, *36*, 6844.
(9) Heilmann, A. *Polymer Films with Embedded Metal Nanoparticles*; Springer, Berlin, 2003.
(10) Xie, X. L.; Mai, Y. W.; Zhou, X. P. *Mater. Sci. Eng. Res.* **2005**, *49*, 89.
(11) Bernholc, J.; Brenner, D.; Nardelli, M. B.; Meunier, V.; Roland, C. *Annu. Rev. Mater. Res.* **2002**, *32*, 347.
(12) Fragiadakis, D.; Pissis, P.; Bokobza, L. *Polymer* **2005**, *46*, 6001.
(13) Hooper, J. B.; Schweitzer, K. S. *Macromolecules* **2005**, *38*, 8850.
(14) Böhning, M.; Goering, H.; Hao, N.; Mach, R.; Schönhals, A. *Polym. Adv. Technol.* **2004**, *16*, 262.
(15) Böhning, M.; Goering, H.; Fritz, A.; Brzezinka, K. W.; Turky, G.; Schönhals, A.; Schartel, B. *Macromolecules* **2005**, *38*, 2764.
(16) Phillips, S. H.; Haddad, T. S.; Tomczak, S. J. *Curr. Opin. Solid State Mater. Sci.* **2004**, *8*, 21.
(17) Joshi, M.; Botola, B. S. *J. Macromol. Sci. C* **2004**, *44*, 389.
(18) Lichtenhan, J. D.; Schwab, J. J.; Reinerth, W. A. *Chem. Innovations.* **2001**, *31*, 3.
(19) Blanski, R. L.; Phillips, S. H.; Chaffee, K.; Lichtenhan, J. D.; Lee, A.; Geng, H. P. *Mater. Res. Symp. Proc.* **2000**, *628*, cc6.27.
(20) Li, G. Z.; Wang, L. C.; Toghiani, H.; Daulton, T. L.; Koyama, K.; Pittman, C. U. *Macromolecules* **2001**, *34*, 8686.
(21) Schiraldi, D.; Iyer, S.; Bu-Ali, A. F.; Gonzalez, R. I.; Kumar, S.; Zeng, J. J. *Abstr. Pap., Am. Chem. Soc.* **2003**, *226*, U505.
(22) Schiraldi, D.; Zeng, J. J.; Kumar, S.; Iyer, S.; Dong, F. J. *Abstr. Pap., Am. Chem. Soc.* **2003**, *225*, U59.
(23) Blanski, R. L.; Phillips, S. H.; Lee, A. J. *Abstr. Pap., Am. Chem. Soc.* **2001**, *221*, U334.
(24) Kopesky, E. T.; Haddad, T. S.; McKinley, G. H.; Cohen, R. E. *Polymer* **2005**, *46*, 4743.
(25) Kopesky, E. T.; Haddad, T. S.; Cohen, R. E.; McKinley, G. H. *Macromolecules* **2004**, *37*, 8992.
(26) Joshi, M.; Botola, B. S.; Simon, G.; Kukaleva, N. *Macromolecules* **2006**, *39*, 1839.
(27) Kopesky, E. T.; McKinley, G. H.; Cohen, R. E. *Polymer* **2006**, *47*, 299.
(28) Zhao, Y. Q.; Schiraldi, D. A. *Polymer* **2005**, *46*, 11640.
(29) Capaldi, F. M.; Rutledge, G. C.; Boyce, M. C. *Macromolecules* **2005**, *38*, 6700.
(30) McCrum, N. G.; Read, B. E.; Williams, G. *Anelastic and Dielectric Effects in Polymeric Solids*; Wiley, New York, 1967 (reprinted by Dover Publications, 1991).
(31) Pötschke, P.; Abdel-Goad, M.; Alig, I.; Dudkin, S.; Lellinger, D. *Polymer* **2004**, *45*, 8863. Pötschke, P.; Dudkin, S. M.; Alig, I. *Polymer* **2003**, *44*, 5023.
(32) Rikowski, E.; Marsmann, H. C. *Polyhedron* **1997**, *19*, 3357.
(33) Bassindale, A. R.; Chen, H. P.; Liu, Z. H.; MacKinnon, L. A.; Parker, D. J.; Taylor, P. G.; Yang, Y. X.; Light, M. E.; Horton, P. N.; Hursthouse, M. B. *J. Organomet. Chem.* **2004**, *689*, 3287.
(34) Hao, N.; Böhning, M.; Goering, H.; Schönhals, A. To be published.
(35) Schönhals, A. *Molecular Dynamics in Polymer Model Systems* In: *Broadband Dielectric Spectroscopy*; Kremer, F., Schönhals, A., Eds.; Springer: Berlin, 2002; p 225.

(36) Kremer, F.; Schönhals, A. Broadband Dielectric Measurement Techniques. In *Broadband Dielectric Spectroscopy*; Kremer, F., Schönhals, A., Eds.; Springer: Berlin, 2002; p 35.
(37) Schönhals, A.; Hao, N. To be published.
(38) Schaefer, J.; Stejskal, E. O.; Buchdahl, R. *Macromolecules* **1977**, *10*, 384.
(39) Floudas, G.; Higgins, J. S.; Kremer, F.; Fischer, E. W. *Macromolecules* **1993**, *25*, 4955.
(40) Alegría, A.; Mitxelena, O.; Colmenero, J. *Macromolecules* **2006**, *39*, 2691.
(41) Merenga, A. S.; Papdakis, C. M.; Kremer, F.; Liu, J.; Yee, A. F. *Macromolecules* **2001**, *34*, 76.
(42) Pratt, G. J.; Smith, M. J. A. *Polym. Int.* **1997**, *43*, 137.
(43) Havriliak, S.; Negami, S. *Polymer* **1967**, *8*, 161. Havriliak, S.; Negami, S. *J. Polym. Sci. C* **1966**, *14*, 99.
(44) Schönhals, A.; Kremer, F. Analysis of Dielectric Spectra. In *Broadband Dielectric Spectroscopy*; Kremer, F., Schönhals, A., Eds.; Springer: Berlin, 2002; p 59.
(45) Vogel, H. *Phys. Z.* **1961**, *22*, 645. Fulcher, G. S. *J. Am. Ceram. Soc.* **1925**, *8*, 339. Tammann, G.; Hesse, W. Z. *Anorg. Allg. Chem.* **1926**, *156*, 245.
(46) Donth, E. *Relaxation and Thermodynamics in Polymers-Glass Transition*; Akademie-Verlag: Berlin, 1992.
(47) Donth, E.; Huth, H.; Beiner, M. *J. Phys.: Condens. Matter*. **2001**, *13*, L451.
(48) Xiao, C.; Wu, J.; Yee, A. F.; Xie, L.; Gidley, D.; Ngai, K. L.; Rizos, A. K. *Macromolecules* **1999**, *32*, 7913.
(49) Shuster, M.; Narkis, M.; Siegmann, A. *Polym. Eng. Sci.* **2004**, *34*, 1613.

MA070036C